Available online at www.sciencedirect.com

ScienceDirect

Ceramics International 40 (2014) 1139–1146

CERAMICS INTERNATIONAL

www.elsevier.com/locate/ceramint

Preparation and characterization of poly(vinyl butyral) electrospun nanocomposite fibers reinforced with ultrasonically functionalized sepiolite

Somaya Ahmed Ben Hassan, Dušica B. Stojanović*, Aleksandar Kojović, Ivona Janković-Častvan, Djordje Janaćković, Petar S. Uskoković, Radoslav Aleksić

Faculty of Technology and Metallurgy, University of Belgrade, Karnegijeva 4, Belgrade, Serbia

Received 15 April 2013; received in revised form 7 June 2013; accepted 28 June 2013
Available online 5 July 2013

Abstract

This study presents an investigation of the effects of the processing conditions on the uniformity, morphology and structure of patterned nanofibrous mats of electrospun poly(vinyl butyral)/sepiolite (PVB/Sep) nanocomposite fibers, which is a novel system for applications in materials for antiballistic protection, biomedical scaffolds and sorption for water purification. Aqueous suspensions of sepiolite exhibit thixotropic behavior because of their fibrous structure, porosity, large specific surface area and the presence of silanol groups on the surface. Functionalization of the sepiolite fibers in an aqueous thixotropic gel was realized on the surface of individual fibers using amino silanes as coupling agents. Different contents (3 wt%, 30 wt% and 50 wt%) of neat and modified sepiolite fibers were dispersed by ultrasonic irradiation in an ethanolic solution of PVB and were used to obtain nanocomposite fibers by electrospinning. The modified PVB/Sep nanocomposite fibers showed a decrease in the mean fiber diameter by about 75% and an increase in the composite storage modulus by about 31% in comparison to the neat PVB fibers. The optimal uniformity of the diameter of the fabricated nanofibers was obtained using a low flow rate (0.5 mL/h), high collector distance (15 cm) and a constant applied voltage of 24 kV. The advantages of the systems lay primarily in improved mechanical properties, which enabled proper manipulation through the achieved mechanical integrity of nanofilter structures in real applications.

Keywords: Sepiolite thixotropic gel; Ultrasonic irradiation; Patterned nanofibrous mats; Dynamic mechanical analysis

1. Introduction

Electrospinning offers a simple method for the production of micro and nanocomposite fibers. Nanocomposite fibers constitute a new class of materials in which polymeric nanofibers are reinforced by dispersed inorganic fillers with at least one dimension in the nanometer-scale. In addition, electrospinning has the following advantages: (a) the diameters of fibrous materials are reduced from micrometers to nanometers; (b) nanofibrous mats can be produced with large surface to mass ratio for better bonding and excellent mechanical strength of the matrix material; (c) nanoparticles can be dispersed in the spin solution and (d) the chemical stability of the nanoparticles is not compromised during spinning and composite fabrication. Electrospun fibers have found increased use in many applications, including multifunctional membranes, biomedical structural elements (scaffolding used in tissue engineering, wound dressing and drug delivery), composite reinforcement and high surface area fabrics for protective clothing and sensors [1]. In particular, thick patterned nanofibrous mats are more valuable in scaffolds, drug carriers, and filters [2].

Nanoparticle-based materials have been attracting growing interest in different fields. However, the main difficulty in working with nanoparticles is their undesirable tendency to form larger particles by agglomeration. To prevent the formation of aggregates, silane coupling agents are extensively used. Silane bonding is one of the most popular surface modifications of

*Corresponding author. Tel.: +381 11 3303754; fax: +381 11 3370387.
E-mail address: duca@tmf.bg.ac.rs (D.B. Stojanović).

0272-8842/$ - see front matter © 2013 Elsevier Ltd and Techna Group S.r.l. All rights reserved.
http://dx.doi.org/10.1016/j.ceramint.2013.06.115

silica, which also has silanol groups on its surface [3]. In the case of sepiolite, a number of chemical modifications of surfaces have been published in scientific papers: modifications with quaternary ammonium salts or amines, or with organosilane, usually in toluene [4–6]. All silane modification processes involving impregnation or suspension in organic solvents have a severe limitation in that the surface modification is not produced on the surface of individual sepiolite fibers but on the external surface of sepiolite aggregates, since highly hydrophilic sepiolite is not finely dispersed such solvents. Surface modification in the form of thixotropic aqueous gels is better than surface grafting in toluene [7]. It is possible to modify mostly individual sepiolite fibers by performing surface modification reactions in thixotropic aqueous gels, which enables the separation of sepiolite aggregates into individual fibers [8].

A wide range of applications may be expected from such functional nanocomposite fibers. Various types of inorganic nanofillers, such as silica, alumina, carbon nanotubes, titania and clay, have been used to produce polymer/inorganic nanofibers and to improve thermo-mechanical properties. Composite nanofibrous mats were prepared from thermoplastic polyurethane/silica nanoparticles, in which gold nanoparticles were used as silica carriers, adsorbed using prior treatment with 3-aminopropyltriethoxysilane, demonstrating that the composite fibers could be used as functional fibers [9]. Nanofibers having an α-alumina structure are excellent candidates for use as reinforcements for polymer matrix composites, as well as to prepare non-woven products having good chemical stability [10,11]. Well-dispersed multi-walled carbon nanotube (MWNT)/PVB nanocomposite fibers were prepared by electrospinning, with enhanced electrical, mechanical, and thermal properties [12]. Photocatalyst TiO_2 nanotubes were obtained by calcination of poly(vinyl alcohol) (PVA)–titanium compound hybrid nanofibers as precursor [13]. The incorporation of clay nanolayers increased the dimensional stability, as well as the thermal and mechanical properties of the functional fibers compared with other fillers due to their layered structure. Most functional clay nanofibers exhibit these improvements in performance at relatively low loadings, which causes a decrease in the mean diameter of the nanocomposite fibers [14].

The approach that was adopted in this study was to include neat and modified sepiolite fibers directly into electrospun fibers from PVB solutions, thus circumventing the problem of fiber aggregation. In the present study, the ultrasonic irradiation technique was used for modification and dispersion of sepiolite fibers into large surface area composite nanofibrous mats. Furthermore, the incorporation of sepiolite nanofibers can change the thermo-mechanical properties of patterned nanofibrous mats. To the best of our knowledge, the selected sepiolite/PVB nanocomposite system has not been previously reported in the literature.

2. Materials and methods

PVB is a resin usually used for applications that require strong binding, optical clarity, adhesion to many surfaces, toughness and flexibility. It is prepared from poly(vinyl alcohol) by reaction with butyraldehyde. PVB (Mowital B75H, dynamic viscosity of 5 wt% solution in ethanol 160–260 mPa s) was purchased from Kuraray. The experiments were performed with 10 wt% ethanolic solution of PVB [15].

Natural sepiolite (Tolića kosa, Serbia) with a specific surface area of 292 m^2/g (BET surface area measurements) was used as a reinforcement filler for nanocomposite fibers in order to influence their fibrous morphology and low production cost. Sepiolite was ultrasonicated (Sonics Vibra Cell, VCX 750, 19 mm Ti horn, 20 kHz) for 20 min in water to disintegrate bundles and dried for 2 h in an oven at 100 °C. The isolated fibers were treated with γ-aminopropyltriethoxysilane (Dynasylan®AMEO, Evonik–Degussa). The sepiolite (Sep) fibers were modified with AMEO silane (5.4 g/4.0 g Sep) by ultrasonic irradiation (20 min) of an aqueous sepiolite gel. The modified sepiolite fibers were dried in an oven at 100 °C overnight, centrifuged (3000 rpm, 15 min), washed with dichloromethane at least five times to remove the excess AMEO silane and, finally, dried under vacuum at 100 °C for 12 h. The neat and the modified sepiolite fibers were added into ethanolic PVB solution and ultrasonically irradiated for 15 min and then stirred continuously for 24 h.

Subsequently, sepiolite filled composite fibers were produced by the electrospinning technique. The electrospinning apparatus (Electrospinner CH-01, Linari Engineering) consisted of a 20 ml plastic syringe with a metallic needle of 0.8 mm inner diameter placed on the syringe pump (R-100E, RAZEL Scientific Instruments) and a high-voltage power supply (Spellman High Voltage Electronics Corporation, Model: PCM50P120). A set of experiments was performed using a 3 wt% suspension of neat sepiolite under applied voltages of $V=16$, 20, 24, 28 and 30 kV with flow rates $Q=0.2$, 0.5 and 1 mL/h. Another experimental set was performed at a flow rate $Q=0.5$ mL/h, while the voltage was held at $V=24$ kV, using 3 wt%, 30 wt% and 50 wt% suspensions of neat and modified sepiolite nanofibers. The tip-to-collector distance was $h_1=15$ cm in all cases. Tip was set vertically above the collector. Fibers were electrospun at room temperature with deposition time of 2 h. The electrospun fibrous mats of the PVB/Sep fibers were collected on an alkaline-resistant fiberglass mesh in the form of patterned nanofibrous mats and kept in air for 15 h to dry.

The following instruments were used for characterization of the neat, modified sepiolite and electrospun nanofibrous mats. Fourier transform infrared (FTIR) spectra of the neat, modified sepiolite fibers and AMEO silane in KBr pellets were obtained in the transmission mode between 400 and 4000 cm^{-1} with a resolution of 4 cm^{-1} using a BOMEM spectrophotometer (Hartmann & Braun, MB-series). Nitrogen adsorption–desorption isotherms were determined using Micromeritics ASAP 2020 instrument. The sepiolite samples were degassed at 150 °C for 10 h under reduced pressure. The specific surface area of samples was calculated using the Brunauer–Emmett–Teller (BET) method from the linear part of the nitrogen adsorption isotherms. The morphology of the as-spun fibers was investigated both by optical microscopy (OLYMPUS CX41) and field emission scanning electron microscopy

(FESEM) on a MIRA3 TESCAN electron microscope at 20 kV. The samples were sputter coated with gold and the surfaces of the mats were analyzed. The fiber diameter distributions of the electrospun fibers were measured using Image-Pro Plus 6.0 analysis software (Media Cybernetics) by manual measurements of the fiber diameters. Dynamic mechanical analysis (DMA, Q800 TA Instruments) of the neat and composite nanofiber patterned mats was conducted in the dual cantilever mode (using a stainless steel sample holder) at a frequency of 1 Hz in the temperature range from 30 °C to 100 °C employing a heating rate of 3 °C/min for the determination of the normalized complex modulus, (E_n^*), loss tangent (tan δ) and the ratio between loss modulus (E'') and storage modulus (E') (Cole–Cole plot).

3. Results and discussion

3.1. Fourier transform infrared measurements

A typical infrared spectrum of the neat sepiolite fibers is shown in Fig. 1(a). The Mg–OH bands are found at 3686 cm^{-1} and 644 cm^{-1}. The Si–O–Si vibrations are present at 1014 cm^{-1} and the vibrations from bonded water are visible at 1659 cm^{-1}, while a shoulder from the Si–O groups appears at 1219 cm^{-1}. There is a broad extended band at 3431 cm^{-1} (zeolitic water) with a smaller band at 3572 cm^{-1} (structural bound water), which suggests that the surface of the sepiolite fibers is covered by a compact layer of zeolitic and adsorbed water. The FTIR spectrum of the pure AMEO silane (Fig. 1(c)) shows a band originating from Si–O–Si vibrations at 1101 cm^{-1}, the strong bands at 2928 cm^{-1} and 2974 cm^{-1} are assigned to the asymmetric, ν_{as}, and symmetric, ν_s, stretching modes of CH_2 groups, and the band at 1593 cm^{-1} may be attributed to $\delta(NH_2)$ deformation vibrations of the NH_2 groups. The infrared spectrum of the modified sepiolite fibers is given in Fig. 1 (b). After modification by AMEO silane, the IR spectrum of sepiolite shows new characteristic absorption bands at 2932 cm^{-1} and 2850 cm^{-1}, which are assigned to the ν_{as} and ν_s of the C–H bond of the $–CH_2–$ group, respectively. In addition, in the IR spectrum of the modified sepiolite fibers, the intensities of the absorption bands from bonded water and structural OH groups are decreased. The decrease in the OH bonds in the modified fibers is assigned to covalent bonding between the sepiolite silanol groups and AMEO silane [16].

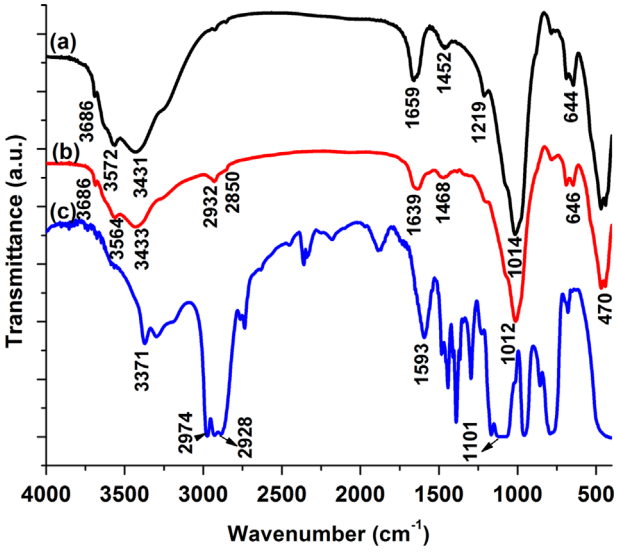

Fig. 1. FTIR spectra of (a) neat sepiolite fibers, (b) modified sepiolite fibers and (c) AMEO silane.

3.2. Fiber dimensions and morphology

Sepiolite is a magnesium hydrated silicate of fibrous morphology, with fine microporous channels of dimensions 0.37–1.06 nm running parallel to the length of the fibers, with the ideal formula $Si_{12}0_{30}Mg_8(OH)_4–(H_2O)_{4.8}H_{20}$. Sepiolite has the highest specific surface area of all the clay minerals, with a high density of silanol groups (Si–OH) on the sepiolite surface [17,18]. The suspension of sepiolite in water (4 wt%) obtained by ultrasonic irradiation (20 min) gave a stable-in-time thixotropic aqueous gel [8], characterized by the formation of a 3D network of sepiolite fibers, which had the highest specific surface area (330 m^2/g, BET surface area measurements) (Fig. 2).

The diameter and morphology of PVB/Sep nanocomposite fibers were studied by optical and scanning electron microscopy (see Supplementary data Figs. S1, S2) to evaluate the relationship of different flow rates, applied voltage, and weight content of neat and modified sepiolite fibers on the fiber diameter and fiber network morphology. Optical microphotographs of the neat PVB and PVB/Sep fibers containing 3 wt% of neat sepiolite are shown in Fig. S1. It is evident from the pictures in Figs. S1 (a–f) that a higher applied voltage, $V=24$, 28 and 30 kV, leads to twisting of the fibers under the same conditions of flow rate $Q=1$ ml/h and sepiolite content 3 wt%.

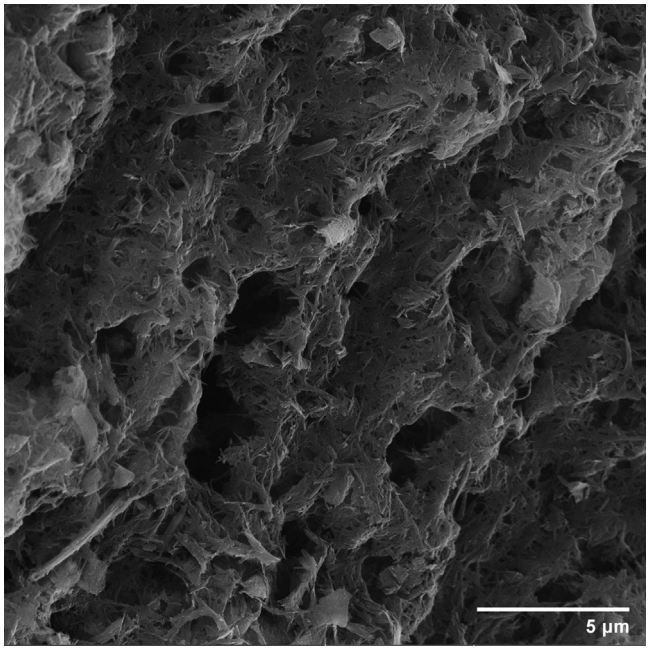

Fig. 2. Sepiolite thixotropic aqueous gel as seen by FESEM.

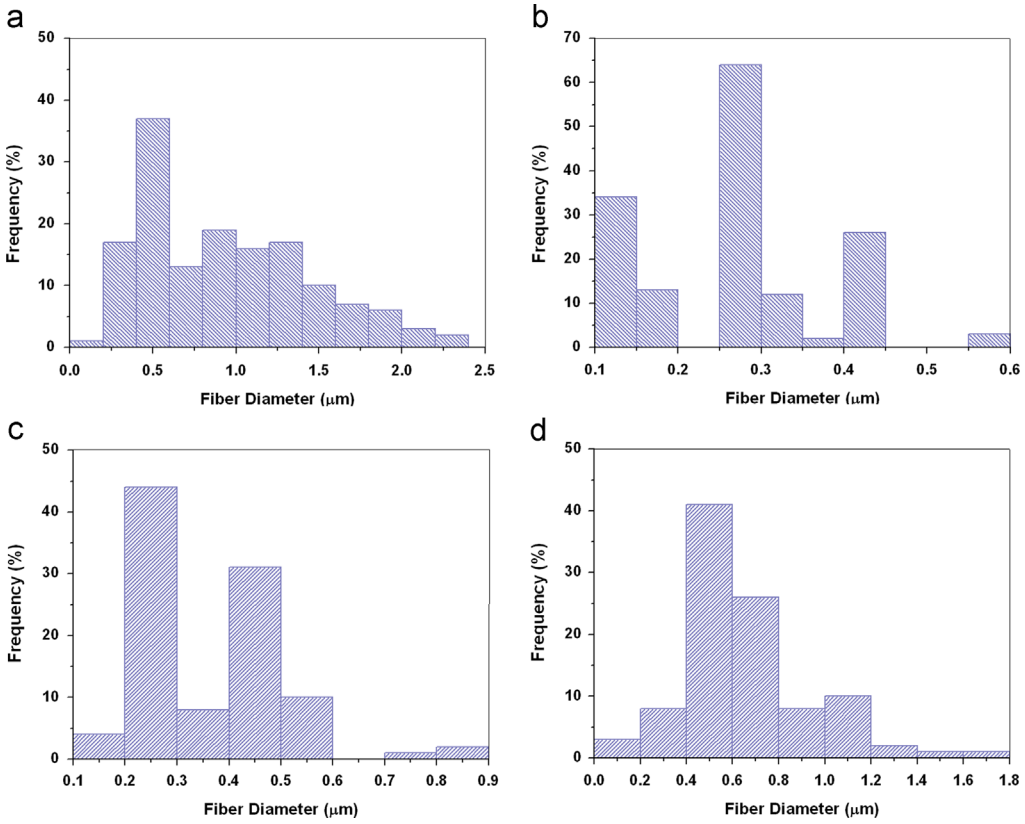

Fig. 3. Histogram of the fiber diameters for electrospun (a) neat PVB fibers and PVB/Sep fibers containing (b) 3 wt%, (c) 30 wt%, and (d) 50 wt% of modified sepiolite using collector distance $h_1 = 15$ cm, flow rate $Q = 0.5$ mL/h and applied voltage $V = 24$ kV.

Table 1
Statistical parameters characterizing the measurement of fiber diameter.

Parameter	PVB fibers	PVB/Sep (3 wt%)	PVB/Sep/AMEO (3 wt%)	PVB/Sep (30 wt%)	PVB/Sep/AMEO (30 wt%)	PVB/Sep (50 wt%)	PVB/Sep/AMEO (50 wt%)
Mean (μm)	0.928	0.777	0.230	0.795	0.368	0.882	0.652
Minimum (μm)	0.149	0.284	0.140	0.284	0.143	0.286	0.144
Maximum (μm)	2.202	1.270	0.599	2.572	0.897	2.020	1.809
Standard deviation (μm)	0.506	0.232	0.108	0.339	0.129	0.337	0.274
Count	150	155	158	156	150	154	150

Fig. S2 shows FESEM images of as-spun PVB/Sep composite fibers obtained by electrospinning 10 wt% PVB solutions containing (a) 3 wt%, (b) 30 wt%, and (c) 50 wt% sepiolite fibers, using a collector distance $h_1 = 15$ cm, a flow rate $Q = 0.5$ mL/h and a constant applied voltage of $V = 24$ kV. For the PVB/Sep fibers containing 30–50 wt% of neat sepiolite fibers, some beaded structure was formed by the large sepiolite agglomerates (Supplementary data, see Fig. S2 (c and e)).

The influence of the sepiolite content on the increase of the mean diameter and of modification with AMEO silane on the decreases of the mean diameters of nanocomposite fibers are shown in Fig. S2 and Fig. 3.

The fiber diameters of the neat PVB fibers were in the range of 0.149–2.202 μm (Table 1, Fig. 3(a)), while the nanocomposite fibers containing 3 wt% modified sepiolite had diameters in range of 0.140–0.599 μm (Fig. 2(b). The mean diameters of the fibers were 0.928 μm for neat fibers and 0.230 μm for silane modified 3 wt% sepiolite nanocomposite fibers. The fiber diameters of the modified fibers containing 30 wt% and 50 wt % sepiolite had diameters in the range 0.143–0.897 μm and 0.144–1.809 μm, respectively, (see Fig. 3 (c and d) and Table 1).

Statistical parameters characterizing fibers diameter distribution are given in Table 1. About 50 fibers were selected for the diameter measurement (using Image-Pro Plus 6.0. analysis software) from three experiments. A significant decrease of the mean fiber diameter of sepiolite composite fibers was evidenced, which appeared for all contents of modified sepiolite fiber (see Fig. 3). Most polymer/clay nanofibers exhibited a decrease in the mean diameter at relatively low loadings, usually less than 5 wt% [19]. The diameter decrease in the nanocomposite fibers may be due to an increase in the conductivity of the PVB solution caused by the clay nanomaterials [20].

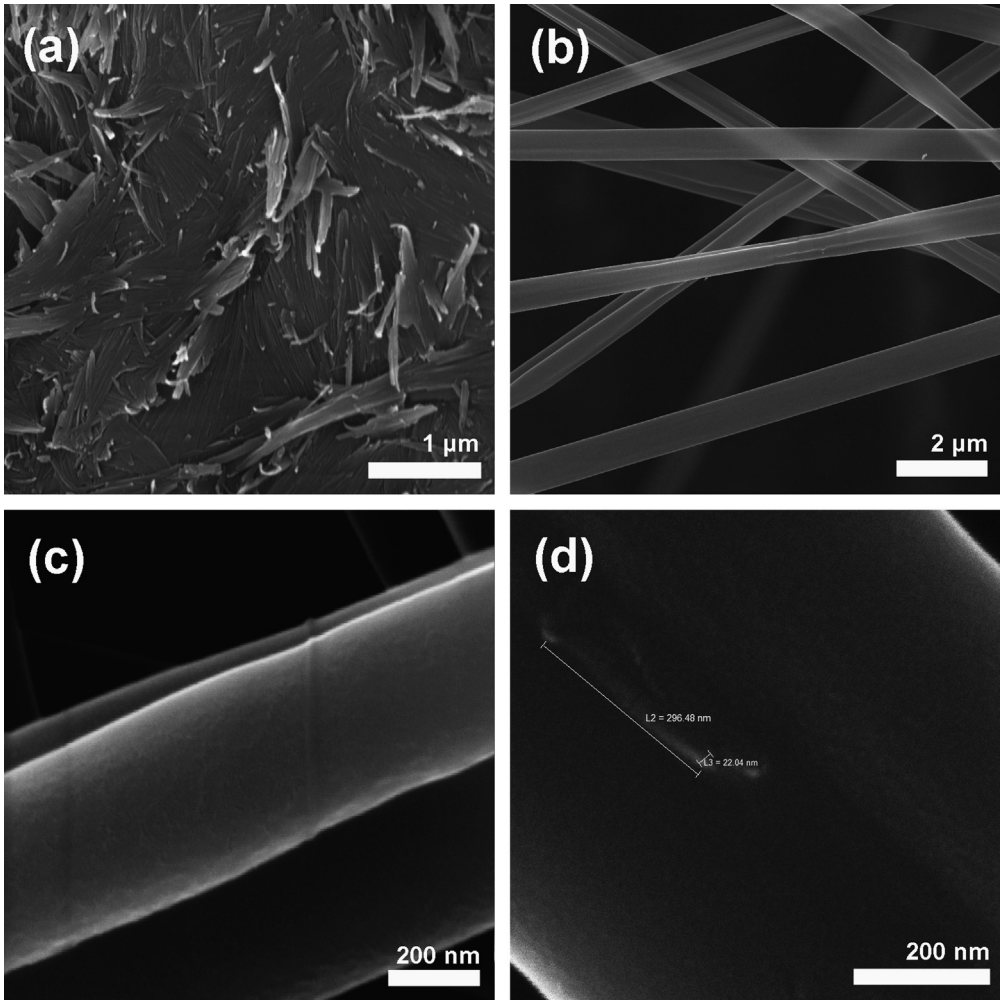

Fig. 4. The morphology of (a) neat sepiolite and (b–d) electrospun PVB/Sep fibers containing 3 wt% of modified sepiolite.

As shown in Fig. 4(a), the neat sepiolite formed aggregates by surface interaction between individual fibers. The as-spun PVB/Sep fibers containing 3 wt% of modified sepiolite fiber had a smooth fibrous structure without beads (Fig. 4(b–d)), which suggested that the modified sepiolite fibers were well-dispersed in the spinning solution. It is shown that the diameter of composite nanofibers is highly dependent on the sepiolite modification technique as well as on electrospinning process (see Supplementary data Fig. S2, Table 1). The technique of electrospinning could also be used in order to improve the dispersion of sepiolite aggregates [17]. It was found that the sepiolite fibers were well-dispersed within the composite fibers and were oriented along the fiber axis (Fig. 4(d)) with a fiber length and diameter of 296 nm and 22 nm, respectively.

3.3. Dynamic mechanical analysis (DMA)

Dynamic mechanical analysis is a method that measures the mechanical properties of a material as a function of the oscillation frequency and the temperature. DMA characterization, gives strength values that are in the form of the complex modulus, E^*, which is given by $E^*=E'+iE''$, where E' is the storage modulus $(E'=|E^*|\cos\delta)$ and E'' $(E''=|E^*|\sin\delta)$ is the loss modulus. Since the samples have viscoelastic properties containing both an elastic part and viscous part, the complex modulus is the sum of the moduli from these two parts. The complex modulus E^* is calculated from the measured data and the sample geometry:

$$E^*_{\text{dual}\times\ \text{cantilever}} = \frac{l^3}{16\ b\ h^3}\frac{F}{A} \tag{1}$$

where: l—sample length; b—sample width; h—sample thickness; F—force; and A—deflection [21]. The ratio between E' and E'', the so called tan δ, shows the loss of energy in the form of heat resulting from the viscoelastic properties of the samples. The loss factor (tan δ) is given by:

$$\tan\ \delta = \frac{E''}{E'} \tag{2}$$

Structural changes of patterned nanofibrous mats after sepiolite addition to polymeric matrices can be studied using the Cole–Cole method. The dynamic mechanical properties when examined as a function of the oscillatory frequency and the temperature are represented on the Cole–Cole complex plane [22]:

$$E = f(E') \tag{3}$$

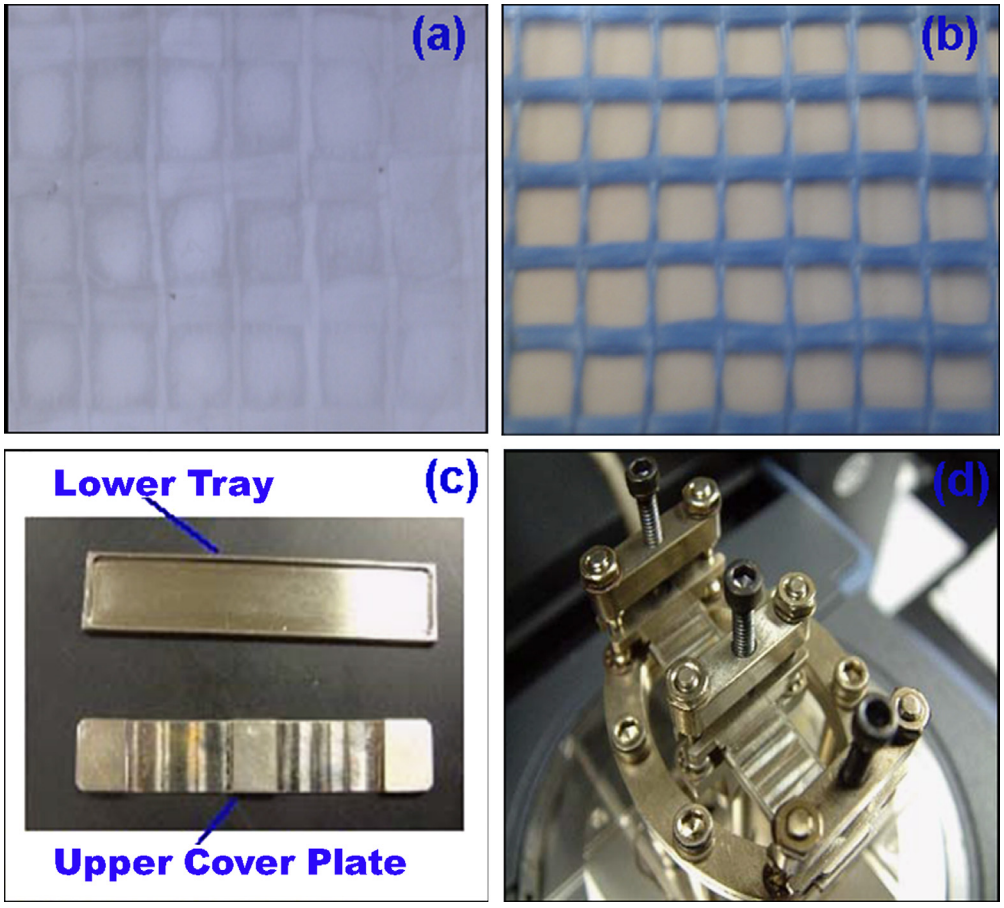

Fig. 5. Photograph of patterned nanofibrous mats (a) collected on a fiberglass mesh (b) using a stainless steel sample holder (c) in the dual cantilever mode (d).

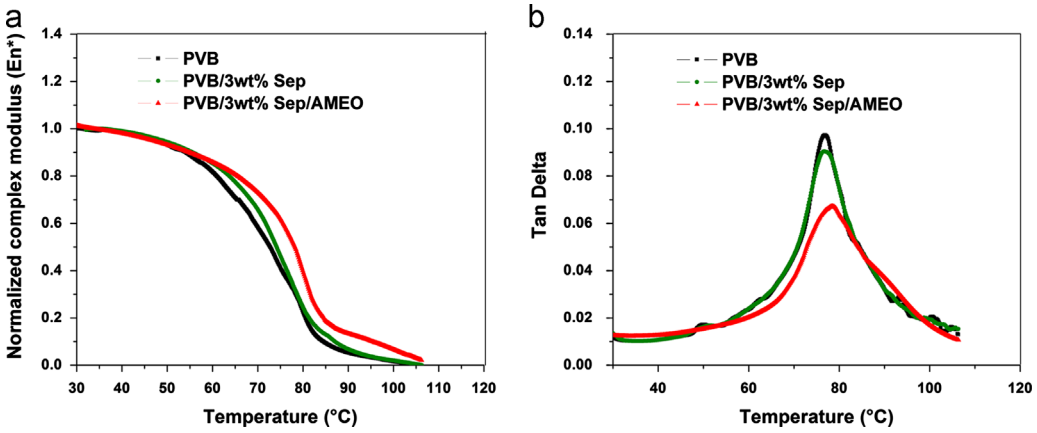

Fig. 6. (a) E_n^* and (b) tan δ vs. temperature curves for patterned nanofibrous mats.

In the present case, DMA was used to determine E_n^*, tan δ and the Cole–Cole plot of the patterned nanofibrous mats consisting of multiple layers of a nanofiber-pattern (Fig. 5(a)). Fig. 5 (c and d) shows the details of the sample holder for DMA characterization. The sample holder is a uniquely designed lower tray and upper cover plate assembly for containing patterned nanofibrous mats. Originally, the method was designed for pharmaceutical powder testing in order to provide powder manufacturers with valuable information related to the glass transition of powder components, usually the active substance and surfactant. This method was extended to include the testing of patterned nanofiber mats in order to extract the properties of materials and avoid possible influences of boundary conditions, such as clamping in the manipulation of the nanofiber mats [23,24]. However, to the best of our knowledge, the present study is the first study in

which DMA was applied to analyze complex nanofibrous materials. DMA of patterned nanofibrous mats was established using the stainless steel sample holder loaded in a DMA Q800 instrument [25]. The clamp was used in conjunction with a 35 mm dual cantilever clamp (adapted from the TA Q800 operator's manual). The patterned mats were cut to the dimensions of the sample holder (approximately 60 mm × 13 mm × 1 mm, ≈100 mg) (see Fig. 5). The employment of the stainless steel sample holder enabled the characterization of the glass transition temperature with temperature change by observing the signal change of the calculated normalized complex modulus, (E_n^*) (Fig. 6(a)).

This normalized complex modulus, presents the ratio of the complex modulus within a sample set to the value of the maximum modulus in the same data set. However, it should be noted that the E' and E'' values obtained using the sample holder accessory are only qualitative (adapted from TA Q800 operator's manual), but the ratio between E'' and E' (Cole–Cole plot) [22] are quantitative. Since tan δ is geometry-independent, structural information at the corresponding temperatures could be obtained using this accessory.

The E_n^* values of the electrospun nanofibrous mats and composite nanofibrous mats as a function of temperature are presented in Fig. 6 (a), which shows a significant reduction in the modulus with temperature. The E_n^* values of the composite nanofibrous mats showed an increase at higher temperatures compared to the pure polymer nanofibrous mats (Fig. 6(a) and Table 2).

The composite nanofibrous mats with AMEO-modified sepiolite showed significant increase in E_n^* at 75 °C (around the T_g temperature of pure PVB) [26]. This indicates an efficient stress transfer between the polymer matrix and the modified sepiolite fibers in the composite nanofibrous mats. The glass transition temperature was defined as the onset temperature of the E_n^* and tan δ peaks. The T_g and tan δ vs. temperature plots of the curves for the patterned nanofibrous mats are presented in Fig. 6(b). The incorporation of neat sepiolite had a modest effect on the T_g and tan δ values. The increase of the T_g and the addition of neat sepiolite fibers reduced the tan δ values of the patterned nanofibrous mats by restricting the movement of polymer molecules and established hydrogen bonding with the silanol groups of the sepiolite surface and OH groups of PVB. The tan δ values of the composite nanofibrous mats were significantly lowered with AMEO silane grafting (0.067). The decrease of the tan δ value is a measure of enhanced interfacial bond strength and adhesion between the polymer matrix and the modified sepiolite fibers.

Table 2
E_n^*, T_g and tan δ peak temperature of patterned nanofibrous mats obtained from DMA.

Sample	E_n^* (at 75 °C)	T_g (°C) (from E_n^*)	T_g (°C) (from tan δ)	Tangent delta (tan δ)
PVB	0.416	69.3	76.9	0.097
PVB/3 wt% Sep	0.466	70.2	77.4	0.090
PVB/3 wt% Sep/AMEO	0.601	72.9	79.1	0.067

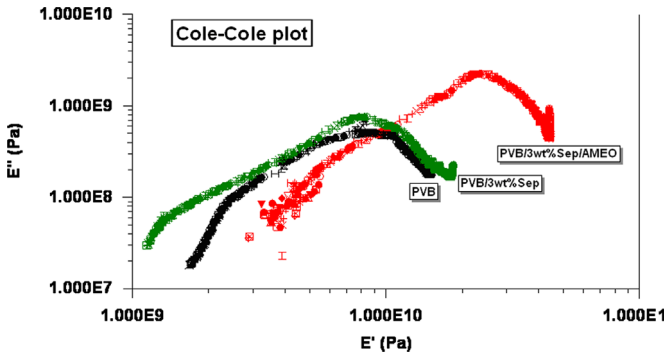

Fig. 7. Cole–Cole plot for patterned nanofibrous mats.

The effect of interface modification between sepiolite fibers and polymer matrix was also confirmed by the Cole–Cole plot in Fig. 7, where the loss modulus data log E'' are plotted as a function of the storage modulus log E'. It is used to examine the structural changes occurring in neat PVB nanofibrous mats and composite nanofibrous mats before and after incorporation of modified sepiolite into the polymeric matrices. The imperfect circles indicate heterogeneity of the hybrid system and favorable amino-modified fibers/polymer bonding.

4. Conclusions

The effects of operating parameters including applied voltage, flow rate and constant tip–target distance on the morphology of electrospun PVB/Sep nanocomposite fibers were systematically evaluated. The modification of the sepiolite thixotropic gel with the AMEO silane led to a better dispersion and deagglomeration of the sepiolite inside the nanocomposite fibers. The composite nanofibers with 3 wt% sepiolite had a mean diameter of 230 nm. The presented dynamic mechanical analysis of the patterned nanofibrous mats is a new method for the characterization and the determination of thermo-mechanical properties. Future research will focus on the preparation of composite nanofibrous mats with higher sepiolite contents and, due to favorable sepiolite properties (sorption, biocompatibility), their applications in antiballistic protection, water purification and biomedical scaffold fabrication will be examined.

Acknowledgments

The authors wish to acknowledge the financial support from the Ministry of Education, Science and Technological Development of the Republic of Serbia through Project nos. TR 34011 and III 45019.

Appendix A. Supporting information

Supplementary data associated with this article can be found in the online version at http://dx.doi.org/10.1016/j.ceramint.2013.06.115.

References

[1] S. Ramakrishna, K. Fujihara, W.E. Teo, T.C. Lim, Z. Ma, Introduction to Electrospinning and Nanofibers, World Scientific, Singapore, 2005.

[2] J. Lee, S.Y. Lee, J. Jang, Y.H. Jeong, D.-W. Cho, Fabrication of patterned nanofibrous mats using direct-write electrospinning, Langmuir 28 (2012) 7267–7275.

[3] D. Stojanovic, A. Orlovic, S. Markovic, V. Radmilovic, P.S. Uskokovic, R. Aleksic, Nanosilica/PMMA composites obtained by the modification of silica nanoparticles in a supercritical carbon dioxide–ethanol mixture, Journal of Materials Science 44 (2009) 6223–6232.

[4] J. Lemic, M. Tomaševic-Canovic, M. Djuricic, T. Stanic, Surface modification of sepiolite with quaternary amines, Journal of Colloid and Interface Science 292 (2005) 11–19.

[5] G. Tartaglione, D. Tabuani, G. Camino, Thermal and morphological characterisation of organically modified sepiolite, Microporous and Mesoporous Materials 107 (2008) 161–168.

[6] V. Marjanović, S. Lazarević, I. Janković-Častvan, B. Potkonjak, Đ. Janaćković, R. Petrović, Chromium(VI) removal from aqueous solutions using mercaptosilane-functionalized sepiolites, Chemical Engineering Journal 166 (2011) 198–206.

[7] X. Liang, Y. Xua, G. Sun, L. Wang, Y. Sun, Y. Sun, X. Qin, Preparation and characterization of mercapto-functionalized sepiolite and their application for sorption of lead and cadmium, Chemical Engineering Journal 174 (2011) 436–444.

[8] N. García, J. Guzmán, E. Benito, A. Esteban-Cubillo, E. Aguilar, J. Santarén, P. Tiemblo, Surface modification of sepiolite in aqueous gels by using methoxysilanes and its impact on the nanofiber dispersion ability, Langmuir 27 (2011) 3952–3959.

[9] X.C. Zhang, Y.Z. Chen, J. Yu, Z.X. Guo, Thermoplastic polyurethane/silica nanocompositefibers by electrospinning, Journal of Polymer Science Part B: Polymer Physics 49 (2011) 1683–1689.

[10] H. Yu, J. Guo, S. Zhu, Y. Li, Q. Zhang, M. Zhu, Preparation of continuous alumina nanofibers *via* electrospinning of PAN/DMF solution, Materials Letters 74 (2012) 247–249.

[11] P. Milanović, M. Dimitrijević, R. Jančić Heinemann, J. Rogan, D.B. Stojanović, A. Kojović, R. Aleksić, Preparation of low cost alumina nanofibers *via* electrospinning of aluminium chloride hydroxide/poly(vinyl alcohol) solution, Ceramics International 39 (2013) 2131–2134.

[12] S. Imaizumi, H. Matsumoto, Y. Konosu, K. Tsuboi, M. Minagawa, A. Tanioka, K. Koziol, A. Windle, Top–down process based on electrospinning, twisting, and heating for producing one-dimensional carbon nanotube assembly, ACS Applied Materials and Interfaces 3 (2011) 469–475.

[13] K. Nakane, N. Shimada, T. Ogihara, N. Ogata, S. Yamaguchi, Formation of TiO_2 nanotubes by thermal decomposition of poly(vinyl alcohol)–titanium alkoxide hybrid nanofibers, Journal of Materials Science 42 (2007) 4031–4035.

[14] Y. Ji, B. Li, S. Ge, J.C. Sokolov, M.H. Rafailovich, Structure and nanomechanical characterization of electrospun PS/clay nanocomposite fibers, Langmuir 22 (2006) 1321–1328.

[15] D. Lubasova, L. Martinova, Controlled morphology of porous polyvinyl butyral nanofibers, Journal of Nanomaterials (2011) http://dx.doi.org/10.1155/2011/292516 Article ID 292516.

[16] H. Chen, M. Zheng, H. Sun, Q. Jia, Characterization and properties of sepiolite/polyurethane nanocomposites, Materials Science and Engineering: A 445–446 (2007) 725–730.

[17] L. Lanotte, C. Bilotti, L. Sabetta, G. Tomaiuolo, S. Guido, Dispersion of sepiolite rods in nanofibers by electrospinning, Polymer 54 (2013) 1295–1297.

[18] Y.P. Zheng, J.X. Zhang, L. Lan, P.Y. Yu, Sepiolite nanofluids with liquid-like behavior, Applied Surface Science 57 (2011) 6171–6174.

[19] S. Zahed, S.S. Naser, The role of Na-montmorillonite on thermal characteristics and morphology of electrospun PAN nanofibers, Fibers and Polymers 11 (2010) 695–699.

[20] J.H. Hong, E.H. Jeong, H.S. Lee, D.H. Baik, S.W. Seo, J.H. Youk, Electrospinning of polyurethane/organically modified montmorillonite nanocomposites, Journal of Polymer Science Part B: Polymer Physics 43 (2005) 3171–3177.

[21] W. Stark, M. Jaunich, Investigation of ethylene/vinyl acetate copolymer (EVA) by thermalanalysis DSC and DMA, Polymer Testing 30 (2011) 236–242.

[22] M. Jawaid, H.P.S. Abdul Khalil, O.S. Alattas, Woven hybrid biocomposites: dynamic mechanical and thermal properties, Composites Part A 43 (2012) 288–293.

[23] P.G. Royall, C.-Y. Huang, S.-W.J. Tang, J. Duncan, G.Van de Velde, M.B. Brown, The development of DMA for the detection of amorphous content in pharmaceutical powdered materials, International Journal of Pharmaceutics 301 (2005) 181–191.

[24] A. Pinheiro, J.F. Mano, Study of the glass transition on viscous-forming and powder materials using dynamic mechanical analysis, Polymer Testing 28 (2009) 89–95.

[25] M.G. Abiad, O.H. Campanella, M.T. Carvajal, Assessment of thermal transitions by dynamic mechanical analysis (DMA) using a novel disposable powder holder, Pharmaceutics 2 (2010) 78–90.

[26] A.M. Torki, D.B. Stojanović, I.D. Živković, A. Marinković, S.D. Škapin, P.S. Uskoković, R.R. Aleksić, The viscoelastic properties of modified thermoplastic impregnated multiaxial aramid fabrics, Polymer Composites 33 (2012) 158–168.